Published OnlineFirst March 7, 2014; DOI: 10.1158/1078-0432.CCR-13-3007

Clinical Cancer Research

Selective JAK2 Inhibition Specifically Decreases Hodgkin Lymphoma and Mediastinal Large B-cell Lymphoma Growth *In Vitro* and *In Vivo*

Yansheng Hao, Bjoern Chapuy, Stefano Monti, et al.

Clin Cancer Res Published OnlineFirst March 7, 2014.

Published OnlineFirst March 7, 2014; DOI: 10.1158/1078-0432.CCR-13-3007

Clinical Cancer Research

Selective JAK2 Inhibition Specifically Decreases Hodgkin Lymphoma and Mediastinal Large B-cell Lymphoma Growth *In Vitro* and *In Vivo*

Yansheng Hao[1], Bjoern Chapuy[1], Stefano Monti[2], Heather H. Sun[3], Scott J. Rodig[3], and Margaret A. Shipp[1]

Abstract

Purpose: Classical Hodgkin lymphoma (cHL) and primary mediastinal large B-cell lymphoma (MLBCL) share similar histologic, clinical, and genetic features. In recent studies, we found that disease-specific chromosome 9p24.1/*JAK2* amplification increased JAK2 expression and activity in both cHL and MLBCL. This prompted us to assess the activity of a clinical grade JAK2 selective inhibitor, fedratinib (SAR302503/TG101348), in *in vitro* and *in vivo* model systems of cHL and MLBCL with defined *JAK2* copy numbers.

Experimental Design: We used functional and immunohistochemical analyses to investigate the preclinical activity of fedratinib and associated biomarkers in cell lines and murine xenograft models of cHL and MLBCL with known 9p24.1/*JAK2* copy number.

Results: Chemical JAK2 inhibition decreased the cellular proliferation of cHL and MLBCL cell lines and induced their apoptosis. There was an inverse correlation between 9p24.1/*JAK2* copy number and the EC_{50} of fedratinib. Chemical JAK2 inhibition decreased phosphorylation of JAK2, STAT1, STAT3, and STAT6 and reduced the expression of additional downstream targets, including PD-L1, in a copy number–dependent manner. In murine xenograft models of cHL and MLBCL with 9p24.1/*JAK2* amplification, chemical JAK2 inhibition significantly decreased JAK2/STAT signaling and tumor growth and prolonged survival. In *in vitro* and *in vivo* studies, pSTAT3 was an excellent biomarker of baseline JAK2 activity and the efficacy of chemical JAK2 inhibition.

Conclusions: In *in vitro* and *in vivo* analyses, cHL and MLBCL with 9p24.1/*JAK2* copy gain are sensitive to chemical JAK2 inhibition suggesting that clinical evaluation of JAK2 blockade is warranted. *Clin Cancer Res; 20(10); 1–10. ©2014 AACR.*

Introduction

Classical Hodgkin lymphoma (cHL) is a tumor of crippled germinal center B cells that lack surface immunoglobulin expression and B-cell receptor-mediated signals and rely on alternative survival pathways (1). These tumors include small numbers of malignant Reed–Sternberg cells within an extensive immune/inflammatory cell infiltrate (1).

The most common subtype of cHL, nodular sclerosing HL (NSHL), shares certain clinical and molecular features with a non-Hodgkin lymphoma, primary mediastinal large B-cell lymphoma (MLBCL) (2). Both of these lymphoid malignancies frequently occur in young adults and often present as localized nodal/anterior mediastinal masses. In earlier studies, we and others defined shared molecular signatures of MLBCL and cHL including constitutive activation of NF-κB (2–4), frequent copy number gains of chromosome 9p24 and JAK2 overexpression (5, 6).

More recently, we integrated high-resolution copy number data with transcriptional profiles in cHL and MLBCL and defined chromosome 9p24.1 amplification as a recurrent alteration in 40% of primary nodular sclerosing Hodgkin lymphomas and 60% of primary MLBCLs (7). In these diseases, the recurrent 9p24.1 amplicon most often includes the immunoregulatory PD-1 ligand genes, *PD-L1* (*CD274*) and *PD-L2* (*PDCD1LG2*), and *JAK2* (7). In cHL and MLBCL cell lines and primary tumors, *JAK2* amplification increased JAK2 protein expression and activity and further induced PD-1 ligand expression via JAK2/STAT signaling (7). In these studies, we treated a panel of cHL and MLBCL cell lines with commercially available tool JAK2 inhibitors and found that these compounds decreased cell line proliferation and PD-L1 expression (7). These preclinical studies provided the rationale for evaluating the activity of clinical grade JAK2 inhibitors in lymphoid malignancies such as cHL and MLBCL with frequent *JAK2* amplification.

Authors' Affiliations: [1]Medical Oncology, Dana-Farber Cancer Institute; [2]Section of Computational Biomedicine, Boston University School of Medicine; and [3]Department of Pathology, Brigham and Women's Hospital, Boston, Massachusetts

Note: Supplementary data for this article are available at Clinical Cancer Research Online (http://clincancerres.aacrjournals.org/).

Corresponding Author: Margaret A. Shipp, Dana-Farber Cancer Institute, 450 Brookline Avenue, Boston, MA 02215-5450. Phone: 617-632-3874; Fax: 617-632-4734; E-mail: Margaret_shipp@dfci.harvard.edu

doi: 10.1158/1078-0432.CCR-13-3007

Published OnlineFirst March 7, 2014; DOI: 10.1158/1078-0432.CCR-13-3007

Translational Relevance

9p24.1/*JAK2* copy gain is one of the most common genetic alterations in cHL and MLBCL. In cHL and MLBCL, *JAK2* amplification increases the expression of JAK2 and the activity of the JAK2/STAT signaling pathway in a copy number–dependent manner. These observations suggest that JAK2 inhibitors, which were originally developed for myeloproliferative disorders with activating *JAK2* mutations, may also be useful in cHLs and MLBCLs with *JAK2* amplification. Herein, we find that cHLs and MLBCLs with 9p24.1/*JAK2* copy gain are particularly sensitive to treatment with the clinical grade JAK2-selective inhibitor, fedratinib, *in vitro* and *in vivo*. Moreover, JAK2 blockade decreases tumor growth, prolongs survival and specifically inhibits JAK2/STAT signaling in murine xenograft models of these lymphoid tumors. These data prompt further consideration of chemical JAK2 blockade as a rational targeted therapy for cHLs and MLBCLs with 9p24.1/*JAK2* amplification.

Clinical grade JAK2 inhibitors including ruxolitinib and fedratinib (SAR302503, previously TG101348) have been extensively analyzed in preclinical models of myeloproliferative disorders with activating *JAK2* mutations (JAK2V617F) and clinical trials of patients with these diseases (8–12). An additional less potent pan-JAK inhibitor, SB1518, has been assessed in myelofibrosis and additional hematologic malignancies (8, 13). Although ruxolitinib has equal efficacy against JAK1 and JAK2 (3 nmol/L IC_{50}) and additional TYK2 inhibition (20 nmol/L IC_{50}), fedratinib is a selective ATP-competitive JAK2 inhibitor (3 nmol/L IC_{50}) with less activity against the other JAK family members, JAK1, TYK2, and JAK3 (8, 10, 14). In initial preclinical murine models of the myeloproliferative disorder, polycythemia vera, fedratinib (TG101348) exhibited clear *in vivo* efficacy with reduction of JAK2V617F-driven disease (10, 11). In subsequent phase I and II clinical trials of fedratinib (TG101348) in myelofibrosis, the selective JAK2 inhibitor was well tolerated and associated with significant reduction in disease burden and durable clinical benefit (12, 15).

Given the importance of JAK2/STAT signaling in cHL and MLBCL, the shared recurrent amplification of 9p24.1/*JAK2* and the utility of fedratinib in additional JAK2-dependent hematopoietic malignancies, we have assessed the *in vitro* and *in vivo* activity of this JAK2-selective inhibitor in cHL and MLBCL.

Materials and Methods

Cell lines

All cell lines were obtained from the DSMZ cell bank. The Karpas 1106P (K1106P) MLBCL cell line and HDLM2 cHL cell line were grown in RPMI-1640 medium (Mediates) supplemented with 20% FBS, L-glutamine, and penicillin/streptomycin. The KMH2, L428, and L1236 cHL cell lines were grown in RPMI-1640 medium (Mediates) supplemented with 10% FBS, L-glutamine, and penicillin/streptomycin and the SUPHD1 cHL cell line was maintained in McCoy's 5A medium (Invitrogen) supplemented with 20% FBS, L-glutamine, and penicillin/streptomycin.

Antibodies and chemicals

The pSTAT1 and pSTAT5 monoclonal antibodies and pJAK2, pSTAT3, and JAK2 antisera were purchased from Cell Signaling. The pSTAT6 antiserum was obtained from ThermoFisher Scientific and the c-MYC and GAPDH antisera and the PIM1 monoclonal antibody were purchased from Santa Cruz Biotechnology. Secondary anti-mouse and anti-rabbit antibodies, conjugated with horseradish peroxidase, were obtained from GE Healthcare. Fedratinib was a gift from Sanofi Aventis.

Cellular proliferation and apoptosis

cHL and MLBCL cell lines were resuspended at a concentration of 2×10^5 cells/mL in culture medium and 50 μL of the cell suspension (1×10^4 cells) was added to each well of a 96-well plate. Thereafter, 50 μL of medium and vehicle (dimethyl sulfoxide) or fedratinib was added to each well in 2-fold serial dilutions. Forty-eight hours later, cellular proliferation was evaluated with the AlamarBlue assay (Invitrogen) according to manufacturer's instructions.

Cells were treated with fedratinib or vehicle for 48 hours and cellular apoptosis was subsequently analyzed by flow cytometry with an Annexin V-APC/DAPI Apoptosis Detection Kit (BD Pharmingen) according to the manufacturer's instructions.

Immunoblotting

After extraction with radioimmunoprecipitation assay buffer, proteins from MLBCL and cHL cell lines were size fractionated with NuPAGE 4% to 12% Bis-Tris gel electrophoresis (Invitrogen), transferred to PVDF membranes (Millipore Corp.), blocked with 5% BSA in 0.1% TBST, incubated with primary antibodies diluted in 3% BSA in 0.1% TBST according to manufacture's instructions, and secondary antibodies conjugated to horseradish peroxidase and then detected with enhanced chemiluminescence (GE Healthcare).

Quantitative reverse-transcription PCR (qRT-PCR)

After cells were treated with vehicle or fedratinib for 24 hours, RNA was extracted with TRizol (Invitrogen) and cDNA was synthesized with the SuperScript III First-Strand Synthesis System Kit (Invitrogen). qRT-PCR was performed using the Applied Biosystem 7300 real-time PCR system with inventoried TaqMan PD-L1 probes (Hs01125299) and internal reference huGAPDH (Applied Biosystem).

Flow cytometry

After treatment with vehicle or fedratinib for 48 hours, 1×10^6 cells were resuspended in 100 μL of PBS, incubated with 2 μg of phycoerythrin-conjugated PD-L1 antibody (Clone 29E.2A3) or isotype control (immunoglobulin G2b κ, BioLegend) for 30 minutes at room temperature,

Published OnlineFirst March 7, 2014; DOI: 10.1158/1078-0432.CCR-13-3007

washed with PBS, and then resuspended in 500 μL of PBS. After staining, 2×10^4 cells were analyzed with a BD FACS Canto flow cytometer (BD Biosciences). FlowJo software (TreeStar) was used to select viable cells by forward and side scatter and generate histograms and median fluorescence intensities.

Intracellular phospho-flow cytometry was performed as previously described (7). In brief, single-cell suspensions were fixed, permeabilized and then stained with either isotype control or Alexa Fluor 647–conjugated phospho-STAT3 (pY705) antibody (BD Bioscience). Phospho staining was normalized to fixed, permeabilized, and isotype-stained cells and fold change was calculated by comparison of median fluorescence intensity values.

Immunohistochemistry

Immunohistochemistry (IHC) for pSTAT1 and pSTAT3 was performed using 4 μm-thick, formalin-fixed, paraffin-embedded tissue sections. Slides were baked, deparaffinized in xylene, passed through graded alcohols, and then antigen retrieved with 1 mmol/L EDTA, pH 8.0 (Invitrogen) in a steam pressure cooker (Decloaking Chamber; BioCare Medical) as per manufacturer's instruction. All further steps were carried out at room temperature in a hydrated chamber. Slides were pretreated with Peroxidase Block (Dako) for 5 minutes to quench endogenous peroxidase activity, and then washed in 50 mmol/L Tris-Cl, pH 7.4. Slides were blocked using Protein Block (Dako) as per manufacturer's instruction, and subsequently incubated with rabbit monoclonal pSTAT1 (clone 58D6, 1:100 dilution for cell lines; Cell Signaling) and rabbit monoclonal pSTAT3 (clone D3A7, 1:200 dilution for cell lines and primary Hodgkin lymphoma; 1:1500 for xenograft studies, Cell Signaling) in diluent (Dako) for 1 hour. Slides were then washed in Tris buffer and treated with anti-rabbit horseradish peroxidase–conjugated antibody (Envision Plus; Dako) for 30 minutes. After further washing, immunoperoxidase staining was developed using a 3,3′-diaminobenzidine (DAB) chromogen (Dako) for 5 minutes. Slides were counterstained with hematoxylin, dehydrated in graded alcohol and xylene, and mounted and coverslipped.

IHC for pJAK2 (clone D3A7, Catalog No. 3771, 1:12.5 dilution for cell lines; Cell Signaling) was performed using 4 μm-thick, formalin-fixed, paraffin-embedded tissue sections on Benchmark XT autostainer (Ventana Medical Systems). UltraView Universal DAB Detection Kit (Catalog No. 760–500; Ventana) was used per manufacturer's instruction. Slides were then washed in soap water and distilled water for post-IHC staining, dehydrated in graded alcohol and xylene, and mounted and coverslipped. Anti-CD20 IHC was performed according to standard protocols (Catalog No. N1502, clone L26; Dako).

In vivo studies

The firefly luciferase and mCherry expressing Karpas 1106P and HDLM2 cell lines were engineered as previously described (16). Subsequently, 5×10^6 viable Karpas 1106P Luc-mCherry cells in 250 μL PBS were injected via the lateral tail veins of 8-week-old male NOD SCID IL2Rγ^{null} mice (Charles River Laboratories). Disease burden was quantified with bioluminescence imaging (IVIS Spectrum, Caliper Life Sciences). Total body luminescence was quantified using the Living Image software package (Caliper Life Sciences) and presented as mean ± SEM with statistical significance determined by Student *t* test. Luc-mCherry HDLM2 cells (1×10^7 cells) in 30% Matrigel were inoculated subcutaneously into mice and tumor size was measured by calipers.

Two weeks following tumor inoculation, animals with established disease documented by imaging (Karpas 1106P) or caliper measurement (HDLM2) were divided into 2 cohorts with equal mean bioluminescence or tumor size and treated twice daily with 120 mg/kg fedratinib or vehicle (0.5% methylcellulose, 0.05% Tween 80) via gavage.

An independent cohort of mice was treated for 5 days with either vehicle or 120 mg/kg fedratinib to assess the pharmacodynamic efficacy of the JAK2 inhibitor. Two hours after the last dose, mice were euthanized and tissues fixed by intracardiac perfusion with 10% formalin. Tumor tissues were harvested and subjected to further fixation overnight in 10% neutral-buffered formalin in preparation for immunohistochemical analyses. All animal studies were performed according to Dana-Farber Cancer Institute Institutional Animal Care and Use Committee approved protocols.

Results

Fedratinib inhibits the proliferation of cHL and MLBCL cell lines in a copy number–dependent manner

We first treated a panel of cHL and MLBCL cell lines of known 9p24.1/*JAK2* copy number with increasing doses of fedratinib (0.313–5 μmol/L) or vehicle alone. The proliferation of cHL and MLBCL cell lines was significantly inhibited by fedratinib and there was an inverse correlation between 9p24.1/*JAK2* copy number and the compound EC_{50}. At a given dose of the JAK2 inhibitor (1.25 μmol/L), there was a significant association between the ranked values of inhibition and copy number gain ($P = 0.009$, all cell lines; $P = 0.019$, cHL cell lines, Kruskal–Wallis test; Fig. 1A and Supplementary Table S1). In addition, fedratinib induced the apoptosis of cHL and MLBCL cell lines and had a more pronounced effect on lines with higher 9p24.1/*JAK2* copy numbers (Fig. 1B). These results indicate that the selective JAK2 inhibitor inhibits the proliferation and induces the apoptosis of cHL and MLBCL cell lines in a *JAK2* copy number–dependent manner.

Fedratinib inhibits JAK2/STAT signaling in cHL and MLBCL cell lines

To more specifically define the downstream consequences of fedratinib treatment in cHL and MLBCL cell lines with defined *JAK2* copy number, we assessed the effect of the compound on the phosphorylation of JAK2 and multiple STAT family members. As anticipated, baseline levels of pJAK2 were most abundant in the cHL cell

Published OnlineFirst March 7, 2014; DOI: 10.1158/1078-0432.CCR-13-3007

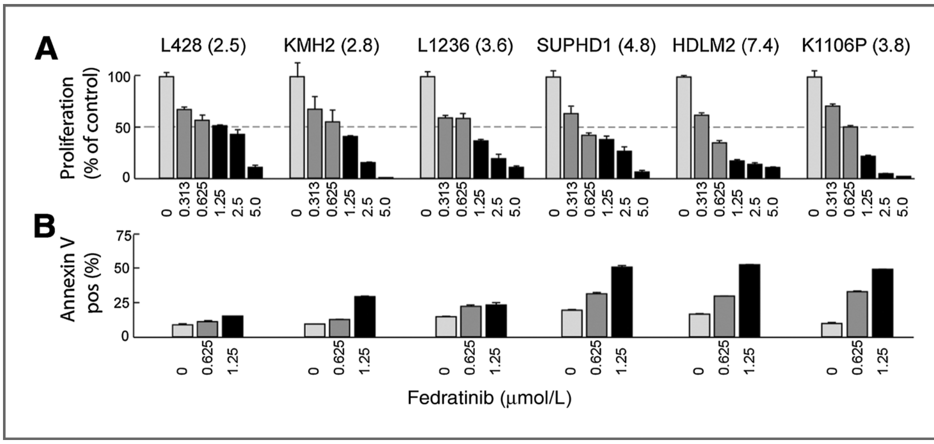

Figure 1. Fedratinib inhibits proliferation and induces apoptosis in cHL and MLBCL cell lines. A, cellular proliferation of cHL cell lines (L428, KMH2, L1236, SUPHD1, and HDLM2) and the MLBCL cell line (K1106P), following treatment with vehicle or fedratinib at indicated concentration for 48 hours. For each cell line, the previously reported 9p24.1/*JAK2* copy numbers (7) are indicated in parenthesis. At a given dose of the JAK2 inhibitor (1.25 μmol/L), a Kruskal–Wallis test was performed to assess the association between the ranked values of inhibition and copy number gain ($P = 0.009$, cHL and MLBCL cell lines; $P = 0.019$, cHL cell lines). B, apoptosis (annexin V^+/$DAPI^-$ plus annexin V^+/$DAPI^+$) of the cHL and MLBCL cell lines following 48 hours of treatment with vehicle or fedratinib. Data in A and B are representative of 3 independent experiments.

lines with highest 9p24.1/*JAK2* copy gain, SUPHD1 and HDLM2 (Fig. 2A). At 24 hours, treatment with fedratinib markedly decreased JAK2 phosphorylation in a dose-dependent manner and cHL and MLBCL cell lines with high 9p24.1/*JAK2* copy number were most sensitive to chemical JAK2 inhibition (Fig. 2A).

Four STAT family members have been reported to be highly active in cHL and MLBCL, STAT1, 3, 5, and 6 (1, 7, 17,

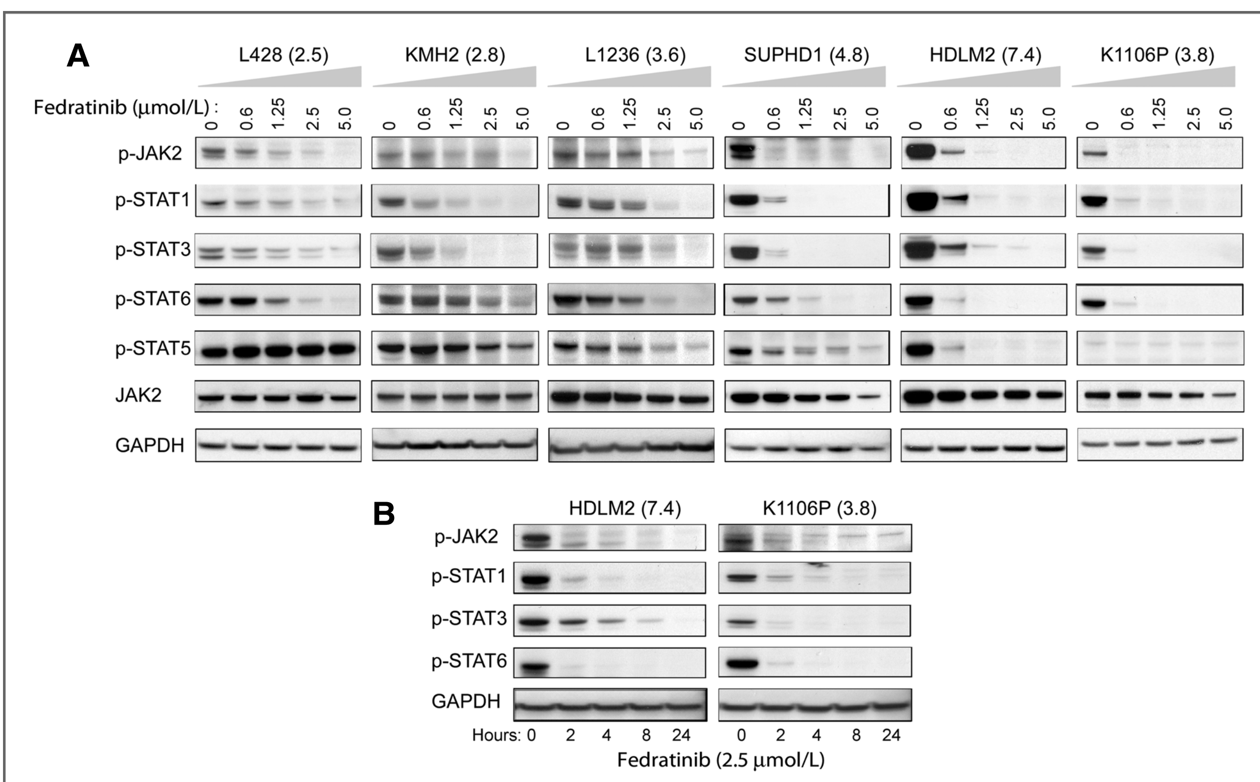

Figure 2. Fedratinib inhibits JAK2/STAT signaling pathway in cHL and MLBCL cell lines. A, Western analysis of pJAK2 and the downstream pSTATs following treatment with vehicle or the indicated concentrations of fedratinib for 24 hours. Total JAK2 and GAPDH are similarly analyzed. B, analysis of pJAK2 and the downstream pSTATs following vehicle or fedratinib (2.5 μmol/L) treatment for 2 to 24 hours. Data in both A and B are representative of 3 independent experiments.

18), prompting us to assess their phosphorylation following fedratinib treatment. The phosphorylation of STAT1, 3, and 6 was dramatically inhibited by chemical JAK2 blockade in a 9p24.1 copy number–dependent manner in the cHL and MLBCL cell lines (Fig. 2A). In contrast, basal pSTAT5 levels were less closely correlated with 9p24.1/*JAK2* copy number and variably responsive to fedratinib treatment (Fig. 2A), potentially reflecting the regulation of STAT5 expression and activity by additional pathways and other JAK family members (19, 20). After demonstrating the 9p24.1/*JAK2* copy number–associated decrease in JAK2 and STAT1, STAT3, and STAT6 phosphorylation following 24 hours of fedratinib treatment, we evaluated the time course of chemical JAK2 inhibition. In cHL and MLBCL cell lines with high 9p24.1/*JAK2* copy number, phosphorylation of JAK2, STAT1, 3, and 6 decreased after only 2 to 4 hours of fedratinib treatment (Fig. 2B). These findings reveal a copy number–dependent, rapid and specific sensitivity of cHLs and MLBCL to chemical JAK2 inhibition.

Development of an immunohistochemical signature of chemical JAK2 inhibition in cHL and MLBCL

Given the close association between sensitivity to fedratinib treatment and decreased phosphorylation of JAK2 and downstream STATs, we sought to develop an immunohistochemical signature of baseline JAK2 activity and response to chemical JAK2 inhibition. In cHL and MLBCL cell lines with high 9p24.1/*JAK2* copy numbers, basal JAK2, STAT1, and STAT3 phosphorylation were readily detectable by IHC and dramatically reduced following 24 hours of fedratinib treatment (Fig. 3A and B). Similar results were obtained after only 4 hours of fedratinib exposure (Supplementary Fig. S1).

In a representative primary cHL with known 9p24.1/*JAK2* amplification, STAT3 phosphorylation was also apparent by IHC (Fig. 3C). These data suggest that pSTAT3 may be a useful marker to assess baseline JAK2/STAT pathway activity and sensitivity to targeted chemical inhibition *in vivo*.

Chemical JAK2 inhibition decreases PD-L1 expression in cHL and MLBCL cell lines

The previously described dependence of PD-L1 expression on JAK2/STAT signaling (7) prompted us to assess PD-L1 transcript abundance and cell surface expression following fedratinib treatment. Chemical JAK2 inhibition reduced PD-L1 transcript levels and cell surface expression in 3 of the 4 cHL cell lines and the MLBCL cell line with high 9p24.1 copy numbers (Fig. 4A and B), underscoring the potential role of fedratinib in modulating PD1 signaling.

Chemical JAK2 inhibition modulates c-MYC and PIM1 expression

We next assessed the consequences of chemical JAK2 inhibition on an additional downstream target of JAK2/STAT signaling, PIM1, and an indirect target of JAK2, c-MYC. In previous studies, JAK2 was reported to phosphorylate the

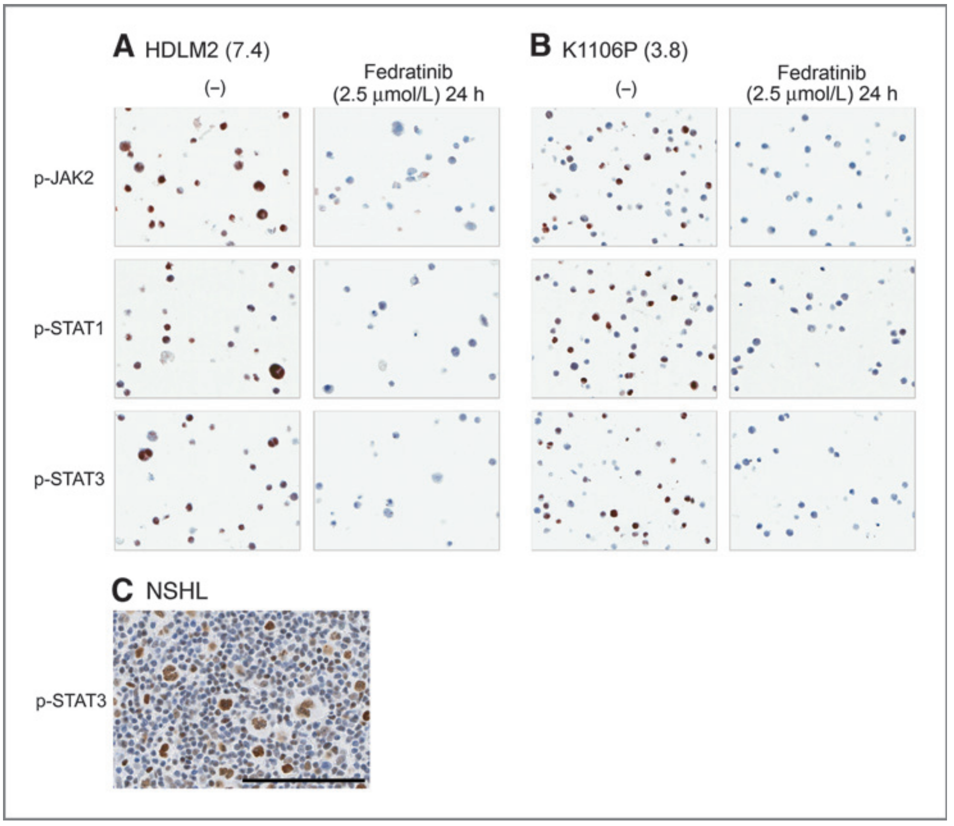

Figure 3. Immunohistochemical signatures of chemical JAK2 inhibition in cHL and MLBCL cell lines. Immunohistochemical analyses of pJAK2, pSTAT1, and pSTAT3 expression in the HDLM2 cHL cell line (A) and the K1106P MLBCL cell line (B) following treatment with vehicle or fedratinib (2.5 μmol/L) for 24 hours (original magnification 400×). C, immunohistochemical analysis of pSTAT3 in a primary cHL with known 9p24.1/*JAK2* amplification (original magnification 400×; scale bar, 100 μm).

Published OnlineFirst March 7, 2014; DOI: 10.1158/1078-0432.CCR-13-3007

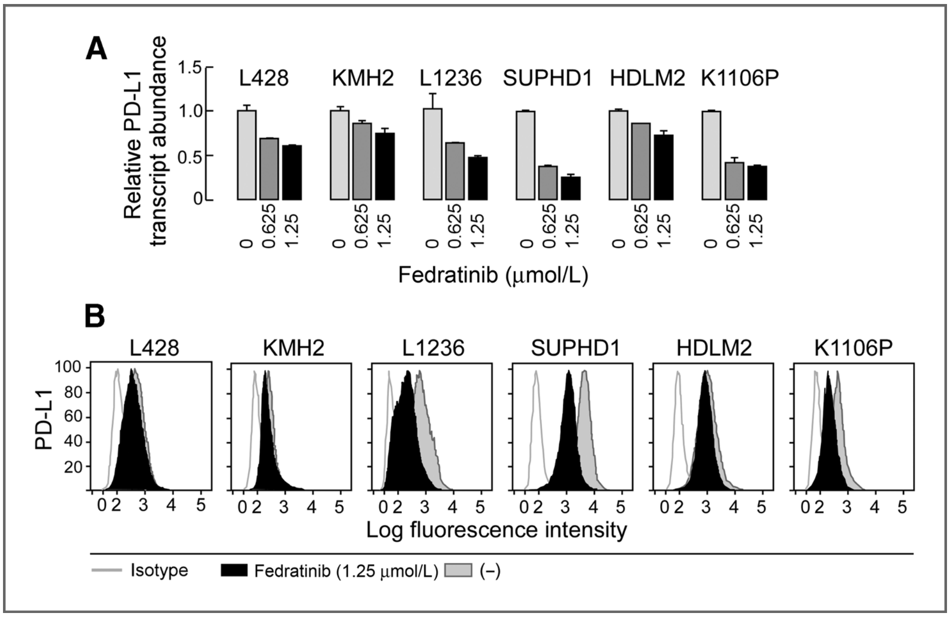

Figure 4. Chemical JAK2 inhibition decreases PD-L1 expression in cHL and MLBCL. A, qRT-PCR analysis of PD-L1 transcript abundance in cell lines treated with vehicle or fedratinib for 24 hours. B, flow cytometric analysis of cell surface PD-L1 expression in cells treated with vehicle or fedratinib for 48 hours. Data in both A and B are representative of 3 independent experiments.

histone H3 tail and block heterochromatin formation and epigenetically modify c-MYC expression (21, 22). We found that fedratinib treatment primarily decreased c-MYC expression in cHL cell lines with higher 9p24.1/*JAK2* copy numbers and modestly reduced c-MYC levels in the MLBCL cell line (Fig. 5).

The *PIM1* oncogene encodes a serine/threonine kinase, which strongly cooperates with c-MYC in murine lymphoma formation (23–25). PIM1 and c-MYC are frequently coexpressed in human hematologic malignancies and PIM1 is a known target of JAK2/STAT signaling (26–28). Consistent with these observations, baseline PIM1 transcript abundance was >3-fold higher in the cHL and MLBCL cell lines with high 9p24.1/*JAK2* copy numbers (Supplementary Fig. S2). Treatment with fedratinib significantly reduced the expression of PIM1 in the cHL lines with the highest 9p24.1/*JAK2* copy number but did not decrease PIM1 expression in the Karpas 1106P MLBCL cell line. These data point to potential differences in the downstream targets of chemical JAK2 inhibition in cHLs and MLBCLs with *JAK2* amplification.

Chemical JAK2 blockade inhibits cHL and MLBCL growth in murine xenograft models

After demonstrating the activity and specificity of fedratinib in *in vitro* assays and determining the optimal dose for *in vivo* studies (Supplementary Fig. S3), we further investigated the antitumor efficacy of the chemical JAK2 inhibitor in murine xenograft models of cHL and MLBCL with 9p24.1/*JAK2* amplification [HDLM2 (cHL) and Karpas 1106P (MLBCL)]. Karpas 1106P cells, which ectopically expressed the firefly luciferase gene, were injected via tail vein and tumor growth was serially monitored via bioluminescence imaging. After documenting established tumors, the MLBCL-bearing mice were treated with fedratinib 120 mg/kg, p.o. twice a day. In an initial cohort of animals, we analyzed pSTAT3 expression as a pharmacodynamic marker following 5 days of treatment. Fedratinib-treated animals had markedly decreased immunostaining of pSTAT3 in lymphomatous Karpas 1106P bone marrow infiltrates (Fig. 6A). Consistent with these initial findings, chemical JAK2 blockade decreased the *in vivo* growth of Karpas 1106P MLBCL (Fig. 6B) and

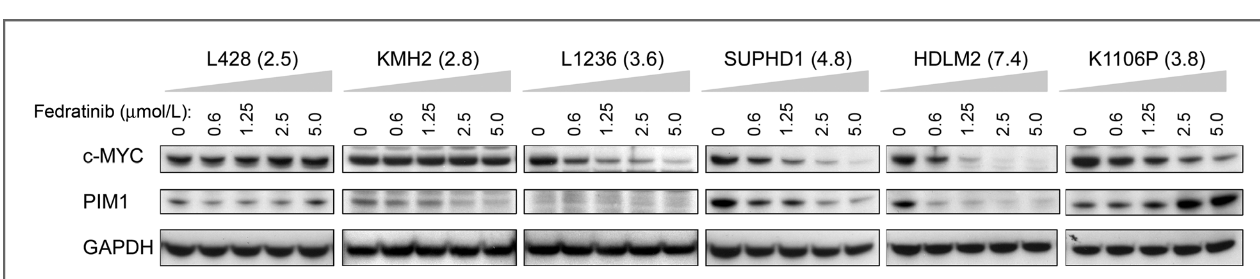

Figure 5. Chemical JAK2 inhibition modulates c-MYC and PIM1 expression in cHL and MLBCL cell lines. Western analysis of c-MYC and PIM1 protein levels in cHL and MLBCL cell lines treated with vehicle or fedratinib at the indicated concentration for 24 hours. Data are representative of 3 independent experiments.

Published OnlineFirst March 7, 2014; DOI: 10.1158/1078-0432.CCR-13-3007

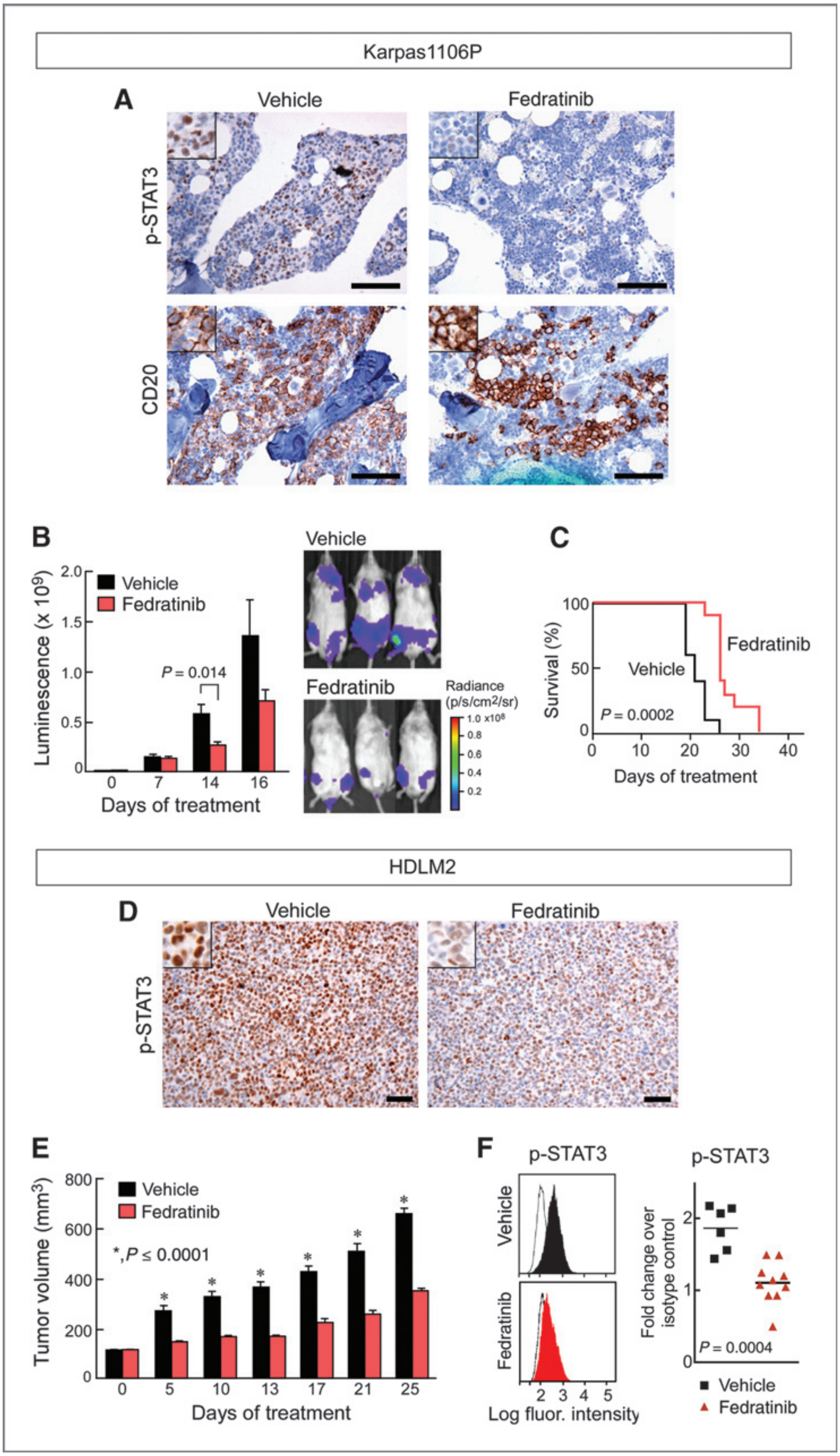

Figure 6. Chemical JAK2 blockage inhibits cHL and MLBCL tumor growth in murine xenograft models. Luciferized Karpas 1106P cells were xenotransplanted into NOD SCID IL2Rγ^{null} (NSG) mice and monitored by bioluminescence imaging. A, immunohistochemical analysis of bone marrow from Karpas 1106P xenograft mice following 5 days treatment with vehicle or fedratinib (4 mice in each group). Infiltrating tumor cells were stained with anti-CD20 and anti-pSTAT3 antibodies, and representative staining is shown at 400× magnification; scale bar, 200 μm. Higher magnification (900×) is shown in insert at upper left corner. B, bioluminescence of vehicle- or fedratinib-treated Karpas 1106P mice (10 mice in each group). Error bars show the SEM. *P* values obtained with Student *t* test. C, survival of Karpas 1106P mice treated with vehicle or fedratinib (10 mice in each group). *P* values obtained with a log-rank (Mantel–Cox) test. Luciferized mCherry+ HDLM2 cells were inoculated subcutaneously into NSG mice. D, immunohistochemical analysis of pSTAT3 expression in a representative tumor mass from HDLM2 xenograft mice following 5 days treatment with vehicle or fedratinib (4 mice in each group). Representative staining is shown at 200× magnification; scale bar, 200 μm. Higher magnification (500×) is shown in insert at upper left corner. E, tumor volume in HDLM2 mice (10 mice in each group) measured by calipers. Error bars show the SEM. F, single cell suspensions were prepared from HDLM2 tumor masses at the end of treatment with vehicle or fedratinib (6 mice in vehicle group and 10 mice in fedratinib group) and residual viable tumor cells were analyzed for pSTAT3 expression by intracellular phosphoflow cytometry. Left, representative pSTAT3 expression in vehicle- and fedratinib-treated tumor cells. Right, comparison of pSTAT3 expression in the vehicle- and fedratinib-treated cohorts. Fold change was calculated by comparing median fluorescence intensity values for pSTAT3 over isotype control for each sample. *P* values in E and F obtained with Student *t* tests.

Published OnlineFirst March 7, 2014; DOI: 10.1158/1078-0432.CCR-13-3007

prolonged the survival of tumor-bearing animals (Fig. 6C, $P = 0.0002$).

In an additional xenograft model, HDLM2 cHL cells were inoculated subcutaneously into the flanks of NSG mice and tumor growth was monitored by external caliper measurements. Treatment was initiated following the establishment of 100 mm^3 tumors. As in the Karpas 1106P MLBCL xenografts (Fig. 6A), 5 days of fedratinib treatment markedly reduced pSTAT3 expression in the HDLM2 cHL xenografts (Fig. 6D). In addition, HDLM2 tumor growth was significantly decreased from 5 days to 25 days of treatment, the last measurable timepoint (Fig. 6E). Thereafter, animals were sacrificed, subcutaneous tumor masses were harvested, and suspended residual tumor cells were analyzed for pSTAT3 expression by intracellular phosphoflow cytometry. In the mCherry-positive residual viable HDLM2 cHL cells, pSTAT3 expression was significantly reduced following fedratinib treatment in comparison to vehicle alone (Fig. 6F). Taken together, these data confirm the prolonged *in vivo* activity of the chemical JAK2 inhibitor and the associated reduction of JAK2/STAT signaling in the MLBCL and cHL xenograft models.

Discussion

Our combined *in vitro* and *in vivo* studies demonstrate that chemical JAK2 inhibition specifically decreases cHL and MLBCL growth in a 9p24.1/*JAK2* copy number–dependent manner. Specifically, we find a copy number–dependent inhibitory effect of the clinical JAK2 inhibitor, fedratinib, on cellular proliferation and viability of cHLs and MLBCLs, JAK2/STAT phosphorylation, and regulation of downstream targets. For the first time, we also document the highly significant *in vivo* efficacy of the JAK2 inhibitor in xenograft models of cHL and MLBCL with 9p24.1/*JAK2* amplification and utilize pSTAT3 as a robust biomarker of JAK2/STAT pathway activity and treatment response. Although clinical development of fedratinib was recently halted because of unanticipated neurotoxicity, additional JAK2 inhibitors are approved for use in other hematologic malignancies and available for analysis in cHL and MLBCL.

Genomic analyses from our group and others highlight the frequency of 9p24.1/*JAK2* copy gain in 40% of primary NSHLs and over 60% of primary MLBCLs (6, 7). The current studies suggest that cHLs and MLBCLs with genetic alterations of *JAK2* will be most sensitive to fedratinib treatment. Although 9p24.1/*JAK2* amplification seems to be the predominant mechanism of deregulating JAK2 activity in cHL and MLBCL, additional alterations have been described. In a series of 131 cHLs, rare *JAK2* rearrangements were identified, including 2 *SEC31A-JAK2* translocations and 2 *JAK2* translocations with unknown partners (29). To date, there is no evidence for JAK2V617F or exon 12 mutations in primary cHL or MLBCL (30, 31). However, additional alterations of negative regulators of JAK2/STAT signaling, such as *PTPN2* and *SOCS1*, have been described. Inactivating *PTPN2* mutations were identified in a single cHL cell line but were not seen in 27 additional primary NSHLs (32). Deletions or inactivating mutations of *SOCS1* are more common in cHL and MLBCL cell lines and primary tumors (33, 34). Given the increased activity of fedratinib in cHLs and MLBCLs with *JAK2* amplification and the additional potential mechanisms of perturbing JAK2/STAT signaling (29, 32–34), it will be important to comprehensively analyze the pathway and its regulators in future clinical trials.

In our current studies, we find pSTAT3 to be a robust biomarker of copy number–dependent JAK2 activity. Our findings are consistent with earlier studies linking numerical aberrations of *JAK2* with increased percentages of STAT3$^+$ tumor cells in cHL and MLBCL (6, 35).

In addition to inhibiting phosphorylation of JAK2-dependent STAT family members, fedratinib decreased the expression of candidate downstream targets, c-MYC and PIM1, in cHL cell lines with high 9p24.1/*JAK2* copy number. However, in the fedratinib-treated MLBCL cell line, c-MYC modulation was less striking and PIM1 was not downregulated. These observations point to potential differences in the signaling and resistance pathways in cHLs and MLBCLs.

In earlier studies, we demonstrated that *JAK2* was co-amplified with *PD-L1* (*CD274*) and *PD-L2* (*PDCD1LG2*) loci as part of the 9p24.1 amplicon, of note because JAK2/STAT signaling further induces the expression of PD-1 ligands (7). The 5′ regulatory region of *PD-L1* includes a classic ISRE/IRF1 module and several degenerate STAT binding sites (7). Previous functional studies confirm that chemical JAK2 inhibition modulates PD-L1 expression via the documented ISRE/IRF1 control element (7). In this study, we extend these findings to demonstrate that the clinical JAK2 inhibitor, fedratinib, decreases PD-L1 transcript abundance and cell surface expression in 3 of 4 cHL lines and the MLBCL cell line with high 9p24.1/*JAK2* copy numbers.

In this study, we also document the *in vivo* efficacy of chemical JAK2 inhibition in 2 xenograft models of tumors with 9p24.1/*JAK2* amplification, Karpas 1106P MLBCL and HDLM2 cHL. In both xenograft models, pSTAT3 was a robust pharmacodynamic biomarker of the efficacy of chemical JAK2 inhibition. Furthermore, chemical JAK2 inhibition significantly decreased tumor growth in both xenograft models and prolonged survival in the model evaluable for this endpoint (Karpas 1106P).

In summary, the current studies support the clinical evaluation of chemical JAK2 blockade in cHL and MLBCL with known 9p24.1/*JAK2* copy gain and further consideration in additional lymphoid tumors with 9p24.1/*JAK2* alterations (6, 36).

Disclosure of Potential Conflicts of Interest

M.A. Shipp has a Commercial Research Grant from Sanofi Aventis. No potential conflicts of interest were disclosed by the other authors.

Authors' Contributions

Conception and design: Y. Hao, B. Chapuy, M.A. Shipp
Development of methodology: Y. Hao, B. Chapuy, M.A. Shipp

Published OnlineFirst March 7, 2014; DOI: 10.1158/1078-0432.CCR-13-3007

Acquisition of data (provided animals, acquired and managed patients, provided facilities, etc.): Y. Hao, B. Chapuy, S.J. Rodig, M.A. Shipp
Analysis and interpretation of data (e.g., statistical analysis, biostatist \ics, computational analysis): Y. Hao, B. Chapuy, S. Monti, H.H. Sun, S.J. Rodig, M.A. Shipp
Writing, review, and/or revision of the manuscript: Y. Hao, B. Chapuy, S.J. Rodig, M.A. Shipp
Administrative, technical, or material support (i.e., reporting or organizing data, constructing databases): H.H. Sun
Study supervision: M.A. Shipp

Grant Support

This work was supported by NIH CA161026, the Miller Family Research Fund, and the Sanofi Aventis Research Agreement.

The costs of publication of this article were defrayed in part by the payment of page charges. This article must therefore be hereby marked *advertisement* in accordance with 18 U.S.C. Section 1734 solely to indicate this fact.

Received November 6, 2013; revised January 21, 2014; accepted February 27, 2014; published OnlineFirst March 7, 2014.

References

1. Kuppers R, Engert A, Hansmann ML. Hodgkin lymphoma. J Clin Invest 2012;122:3439–47.
2. Savage KJ, Monti S, Kutok JL, Cattoretti G, Neuberg D, De Leval L, et al. The molecular signature of mediastinal large B-cell lymphoma differs from that of other diffuse large B-cell lymphomas and shares features with classical Hodgkin lymphoma. Blood 2003;102:3871–9.
3. Rosenwald A, Wright G, Leroy K, Yu X, Gaulard P, Gascoyne RD, et al. Molecular diagnosis of primary mediastinal B cell lymphoma identifies a clinically favorable subgroup of diffuse large B cell lymphoma related to Hodgkin lymphoma. J Exp Med 2003;198:851–62.
4. Tiacci E, Doring C, Brune V, van Noesel CJ, Klapper W, Mechtersheimer G, et al. Analyzing primary Hodgkin and Reed–Sternberg cells to capture the molecular and cellular pathogenesis of classical Hodgkin lymphoma. Blood 2012;120:4609–20.
5. Joos S, Kupper M, Ohl S, von Bonin F, Mechtersheimer G, Bentz M, et al. Genomic imbalances including amplification of the tyrosine kinase gene JAK2 in $CD30^+$ Hodgkin cells. Cancer Res 2000;60: 549–52.
6. Meier C, Hoeller S, Bourgau C, Hirschmann P, Schwaller J, Went P, et al. Recurrent numerical aberrations of JAK2 and deregulation of the JAK2-STAT cascade in lymphomas. Mod Pathol 2009;22: 476–87.
7. Green MR, Monti S, Rodig SJ, Juszczynski P, Currie T, O'Donnell E, et al. Integrative analysis reveals selective 9p24.1 amplification, increased PD-1 ligand expression, and further induction via JAK2 in nodular sclerosing Hodgkin lymphoma and primary mediastinal large B-cell lymphoma. Blood 2010;116:3268–77.
8. Quintqas-Cardama A, Verstovsek S. Molecular pathways: Jak/STAT pathway: mutations, inhibitors, and resistance. Clin Cancer Res 2013;19:1933–40.
9. Verstovsek S, Kantarjian H, Mesa R, Perdanani A, Cortes-Franco J, Thomas D, et al. Safety and efficacy of INCB018424, a JAK1 and JAK2 inhibitor, in myelofibrosis. New Engl J Med 2010;363:1117–27.
10. Wernig G, Kharas MG, Okabe R, Moore SA, Leeman DS, Cullen DE, et al. Efficacy of TG101348, a selective JAK2 inhibitor, in treatment of a murine model of JAK2V617F-induced polycythemia vera. Cancer Cell 2008;13:311–20.
11. Geron I, Abrahamsson AE, Barroga CF, Kavalerchik E, Gotib J, Hood JD, et al. Selective inhibition of JAK2-driven erythroid differentiation of polycythemia vera progenitors. Cancer Cell 2008;13:321–30.
12. Pardanani A, Gotlib JR, Jamieson C, Cortes JE, Talpaz M, Stone RM, et al. Safety and efficacy of TG101348, a selective JAK2 inhibitor, in myelofibrosis. J Clin Oncol 2011;29:789–96.
13. Younes A, Romaquera J, Fanale M, McLaughlin P, Hagemeister F, Copeland A, et al. Phase I study of a novel oral Janus kinase 2 inhibitor, SB1518, in patients with relapsed lymphoma: evidence of clinical and biologic activity in multiple lymphoma subtypes. J Clin Oncol 2012;30:4161–7.
14. Zhou T, Georgeon S, Moser R, Moore DJ, Caflisch A, Hantschel O. Letter to the Editor: specificity and mechanism-of-action of the JAK2 tyrosine kinase inhibitors ruxolitinib and SAR302503 (TG101348). Leukemia Prepublication on-line July 4, 2013 2013:1–4.
15. Talpaz M, Jamieson C, Gabrail N, Lebedinsky C, Gao G, Patki A, et al. Updated results from a randomized phase 2 dose-ranging study of the JAK2-selective inhibitor SAR302503 in patients with intermediate-2 or high-risk myelofibrosis (MF). Haematologica 98;sI, 2013 (abstract S1113).
16. Monti S, Bjoern C, Takeyama K, Rodig SJ, Hao Y, Yeda KT, et al. Integrative analysis reveals an outcome-associated and targetable pattern of p53 and cell cycle deregulation in diffuse large B cell lymphoma. Cancer Cell 2012;22:359–72.
17. Guiter C, Dusanter-Fourt I, Copie-Bergman C, Boulland ML, Le Gouvello S, Gaulard P, et al. Constitutive STAT6 activation in primary mediastinal large B-cell lymphoma. Blood 2004;104:543–9.
18. Skinnider BF, Elia AJ, Gascoyne RD, Patterson B, Trumper L, Kapp U, et al. Signal transducer and activator of transcription 6 is frequently activated in Hodgkin and Reed-Sternberg cells of Hodgkin lymphoma. Blood 2002;99:618–26.
19. Hinz M, Lemke P, Anagnostopoulos I, Hacker C, Krappmann D, Mathas S, et al. Nuclear factor kappaB-dependent gene expression profiling of Hodgkin's disease tumor cells, pathogenetic significance, and link to constitutive signal transducer and activator of transcription 5a activity. J Exp Med 2002;196:605–17.
20. Scheeren FA, Diehl SA, Smit LA, Beaumont T, Naspetti M, Bende RJ, et al. IL-21 is expressed in Hodgkin lymphoma and activates STAT5: evidence that activated STAT5 is required for Hodgkin lymphomagenesis. Blood 2008;111:4706–15.
21. Dawson MA, Bannister AJ, Gottgens B, Foster SD, Bartke T, Green AR, et al. JAK2 phosphorylates histone H3Y41 and excludes HP1α from chromatin. Nature 2009;461:819–22.
22. Rui L, Emre NC, Kruhlak MJ, Chung HJ, Steidl C, Slack G, et al. Cooperative epigenetic modulation by cancer amplicon genes. Cancer Cell 2010;18:590–605.
23. van Lohuizen M, Verbeek S, Scheijen B, Wientiens E, van der Gulden H, Berns A. Identification of cooperating oncogenes in E mu-myc transgenic mice by provirus tagging. Cell 1991;65:737–52.
24. Verbeek S, van Lohuizen M, van der Valk M, Domen J, Kraal G, Berns A. Mice bearing the E mu-MYC and E mu-pim1 transgenes develop pre-B-cell leukemia prenatally. Mol Cell Biol 1991;11:1176–9.
25. Mikkers H, Allen J, Knipscheer P, Romeijn L, Hart A, Vink E, et al. High-throughput retroviral tagging to identify components of specific signaling pathways in cancer. Nat Genet 2002;32:153–9.
26. Miura O, Miura Y, Nakamura N, Quelle FW, Witthuhn BA, Ihle JN, et al. Induction of tyrosine phosphorylation of Vav and expression of Pim-1 correlates with Jak2-mediated growth signaling from the erythropoietin receptor. Blood 1994;84:4135–41.
27. Matikainen S, Sareneva T, Ronni T, Lehtonen A, Koskinen PJ, Julkunen I. Interferon-α activates multiple STAT proteins and upregulates proliferation-associated IL-2Rα, c-MYC, and PIM-1 genes in human T cells. Blood 1999;93:1980–91.
28. Didichenko SA, Spiegl N, Brunner T, Dahinden CA. IL-3 induces a PIM1-dependent anti-apoptotic pathway in primary human basophils. Blood 2008;112:3949–58.
29. Van Roosbroeck K, Cox L, Tousseyn T, Lahortiga I, Gielen O, Cauwelier B, et al. *JAK2* rearrangements, including the novel SEC31A-JAK2 fusion, are recurrent in classical Hodgkin lymphoma. Blood 2011; 117:4056–64.
30. Melzner I, Weniger MA, Menz CK, Moller P. Letter to the Editor: Absence of the JAK2 V617F activating mutation in classical Hodgkin lymphoma and primary mediastinal B-cell lymphoma. Leukemia 2006;20:157–8.
31. Wu D, Lindeman N, Takahashi H, Takeyama K, Harris NL, Pinkus GS, et al. No evidence for the JAK2V617F mutation in primary mediastinal large B-cell lymphoma. Diag Mol Pathol 2009;18:144–9.

Published OnlineFirst March 7, 2014; DOI: 10.1158/1078-0432.CCR-13-3007

32. Kleppe M, Tousseyn T, Geissinger E, Kalender Atak Z, Aerts S, Rosenwald A, et al. Mutation analysis of the tyrosine phosphatase PTPN2 in Hodgkin's lymphoma and T-cell non-Hodgkin's lymphoma. Haematology 2011;96:1723–7.
33. Melzner I, Bucur AJ, Bruderlein S, Dorsch K, Hasel C, Barth TF, et al. Biallelic mutation of SOCS-1 impairs JAK2 degradation and sustains phospho-JAK2 action in the MedB-1 mediastinal lymphoma line. Blood 2005;105:2535–42.
34. Weniger M, Melzner I, Menz C, Wegener S, Bucur AJ, Dorsch K, et al. Mutations of the tumor suppressor gene SOCS-1 in classical Hodgkin lymphoma are frequent and associated with nuclear phospho-STAT5 accumulation. Oncogene 2006;25:2679–84.
35. Holtick U, Vockerodt M, Pinkert D, Schoof N, Stürzenhofecker B, Kussebi N, et al. STAT3 is essential for Hodgkin lymphoma cell proliferation and is a target of tyrophostin AG17 which confers sensitization of apoptosis. Leukemia 2005;19:936–44.
36. Eberle FC, Salaverria I, Steidl C, Summers TA Jr., Pittaluga S, Neeriah SB, et al. Gray zone lymphoma: chromosomal aberrations with immunophenotypic and clinical correlations. Modern Pathol 2011;24: 1586–97.